Research in Astronomy and Astrophysics, 23:015012 (6pp), 2023 January https://doi.org/10.1088/1674-4527/aca4b6

Research on a 3.7-year Quasi-periodic Oscillation for FSRQ J0351-1153

Lin Lu, Wei-Lu Zhou, Guang-Yi Luo, and Bin Sun
Department of Physics, Zunyi Normal University, Zunyi 563002, China; 403285880@qq.com
Received 2022 September 1; revised 2022 October 28; accepted 2022 November 9; published 2022 December 14

Abstract

From the Owens Valley Radio Observatory 40 m radio telescope, we have collected the light curves of the 15 GHz radio band for FSRQ J0153-1153, spanning from 2009 February to 2018 February. The Lomb–Scargle Periodogram method and the Weighted Wavelet Z-transform method are employed to search for the quasi-periodic oscillation (QPO) signal of these data, and the simulation method for the light curve is utilized to estimate the significance level of this QPO signal; thus through these techniques, the QPO signal of 3.7 ± 0.5 yr with a significance level of 3.68σ is revealed for the first time. It is most likely an explanation for the QPO signal that a binary black hole system gives rise to a Newtonian-driven the precession of jet. Based on this assumption, we find that the mass of the secondary black hole in this system may be larger than the mass of the primary black hole; and we estimate the intrinsic QPO of jet precession and the QPO of companion star orbit.

Key words: galaxies: active – methods: data analysis – galaxies: jets

1. Introduction

On cosmological distance scales, active galactic nuclei (AGNs) are extreme objects that demonstrate violent and rapid variability in electromagnetic radiation (Hong et al. 2018). Blazars are a subclass of AGNs and the direction of the jet of blazars points to the observers (Urry & Padovani 1995; Padovani et al. 2016; Xiong et al. 2020). In the center of blazars, there are supermassive black holes (SMBHs) with masses ranging from 10^6 to $10^{10}\,M_\odot$ (Esposito et al. 2015; Gupta et al. 2019). The emission of blazars is dominated by non-thermal radiation (Angel & Stockman 1980; Urry & Padovani 1995; Xiong et al. 2017). Based on the strength of optical emission lines, blazars are classified into two main subclasses: BL Lacertae objects (BL Lacs) and flat-spectrum radio quasars (FSRQs) (Ren et al. 2021a). The equivalent width (EW) of the emission line is above 5 angstrom for FSRQ, whereas the EW of the emission line is below 5 angstrom or no for BL Lacs (Urry & Padovani 1995; Xiong et al. 2017; Hong et al. 2018). In whole bands, there is a double peak structure to the spectral energy distribution (SED) of blazars. Usually, the peaks ranging from X-rays to γ-rays are produced by the inverse Compton (IC) process, whereas peaks ranging from radio to X-rays are produced by the synchrotron radiation of relativistic electron within the jet (Ren et al. 2021a, 2021b). Based on the location of the SED peak, blazars have already been divided into three types: low synchrotron peaked (LSP) ($\nu_{\rm peak} < 10^{14}$ Hz), intermediate synchrotron peaked (ISP) (10^{14} Hz $\leqslant \nu_{\rm peak} \leqslant 10^{15}$Hz), and high synchrotron peaked (HSP) ($\nu_{\rm peak} > 10^{15}$ Hz) (Abdo et al. 2010; Hong et al. 2017; Iyida et al. 2022).

In many bands, blazars show flux variability with timescales ranging from minutes to days, from weeks to years, and even decades. The study of light curves is important for revealing the internal structure, the mass of the central black hole, the radius of the radiation region, and other issues in blazars (Urry & Padovani 1995). In particular, there are blazars with QPO signals. These QPO signals are likely to reflect the periodic physical processes within blazars. However, due to equipment failures, weather conditions and some unavoidable errors, the astronomical observation data will be uneven intervals. Therefore, reliable QPO signals cannot be extracted from such astronomical data by traditional period analysis methods. Therefore, a popular topic in time domain astronomy is how to acquire trustworthy QPO signals. In the previous studies of AGNs, the QPO signals were found to exist in many bands. Many physical models have been proposed to explain these QPO signals. For example, Bhatta (2018) discovered the existence of a 560 day QPO signal in the radio band of Blazar J1043+2408, and based on this QPO signal they discussed the interpretation including supermassive binary black holes, Lense-Thirring precession and jet precession. In 2021, Zhang & Wang (2021) found a 176 day high-confidence QPO signal in the radio band of Radio-loud Narrow-line Seyfert 1 galaxy J0849+5108. They believe that a secular instability in the inner accretion disk or a helical structure in the jet gives rise to this high-confidence QPO signal. In 2021, a 965 day QPO signal was found in the study of Blazar AO 0235+164. The QPO signal was attributed to the helical structure within a jet or the orbital-induced precession of a jet (Tripathi et al. 2021); in study of the radio band of OT 081, Li et al. (2021) found a 850 day QPO signal, which they hypothesized to originate from a

binary supermassive black hole and estimated the intrinsic physical parameters of this system, and they also discussed that this QPO signal originated from the helical motion of the blob in the jet. In particular, some physical properties within blazars can be discussed more deeply through the study of multi-band combination; for instance, the 2 yr QPO signal was found in the study of the multi-band light curve of PG 1553+113 by Ackermann et al. (2015). They discuss several possible physical models that give rise to this QPO signal, such as instability of the pulsational accretion flow with approximating the periodic behavior can explain the modulation of the energy outflow efficiency, non-ballistic hydrodynamic jet precession can explain variations with periods above 1 yr and gravitationally bound supermassive binary black hole systems, the periodic motion of Keplerian orbits may cause periodic accretion perturbations, etc. (Ackermann et al. 2015). These previous studies reflect that the QPO signals at different timescales may be due to different physical processes. Therefore, the QPO signals are important for the study of different physical processes within AGNs. Blazar PKS J0351-1153 (redshift $z = 1.52$, Lee et al. 2017) has been classified as an FSRQ (Healey et al. 2007). Since 2008, this source has been monitored in the 15 GHz. In this work, we search for the QPO signal of this source using the LSP and WWZ methods and estimate the significance level of the QPO signal using the simulation method for light curve. Thus, by means of these techniques we obtain a QPO signal of 3.7 ± 0.5 yr with the significance level of 3.68σ and we believe that it is likely explanation for the potential QPO signal that a system of binary black hole give rises to Newtonian-driven the precession of jet.

In this work, we present our work on a search for the potential QPO signal in radio light curve at 15 GHz of FSRQ J0351-1153. This paper is organized as follows: in Section 2, the LSP method and WWZ method are introduced; in Section 3, we analyze the light curve of this source using two methods, including estimation of significance level of the QPO signal, and the presentation of the analytical results; in Section 4, the origin of the QPO signal is discussed; and in Section 5, some conclusions are summarized.

2. Analysis Method of Astronomical Periodic Signal

2.1. Lomb–Scargle Periodogram (LSP) Method

The periodograms of the non-uniformly time series can be phase-corrected utilizing the LSP method (Lomb 1976; Scargle 1982). As a result, this method is capable of finding quasi-periodic oscillation signals hidden in noise.

Now it is assumed that there is a group of time series with non-uniform sampling interval $x(t_j)$, $j = 1, 2, 3.....,N$ (VanderPlas 2018). The following equation gives the LSP power spectral density of the time series. Its fundamental formulation is:

$$P_x(\omega_j) = \frac{1}{2}\left\{\frac{\sum_{j=1}^{N}[\{x(t_j) - \bar{x}\}\cos(t_j - \tau)]}{\sum_{j=1}^{N}\cos^2[\omega_j(t_j - \tau)]} + \frac{\sum_{j=1}^{N}[\{x(t_j) - \bar{x}\}\sin(t_j - \tau)]}{\sum_{j=1}^{N}\sin^2[\omega_j(t_j - \tau)]}\right\}, \quad (1)$$

In which, f_j is the frequency of the QPO being attempted, in units of $1/\mathrm{day}$ (Ren et al. 2021a, 2021b), and $P_x(\omega_j)$ is the power spectrum ($(\omega_j = 2\pi f_j)$), $\bar{x} = \frac{1}{N}\sum_{j=1}^{N} x_j$ is the average of time series, N is the number of data points and τ is the time-series phase correction:

$$\tan(2\omega_j\tau) = \frac{\sum_{j=1}^{N}\sin^2(2\omega_j t_j)}{\sum_{j=1}^{N}\cos^2(2\omega_j t_j)}, \quad (2)$$

2.2. Weighted Wavelet Z-transform (WWZ) Method

In 1996, Foster developed the WWZ method (Foster 1996a, 1996b). This method is not only applicable to the analysis of periodic signals of astronomical data but also reflects the variation of periodic signals with time. The time series is projected onto three orthogonal normalized basis vector functions using the WWZ method. These are the three basic vector functions: $\varphi_1(t_i) = 1$, $\varphi_2(t_i) = \cos[\omega_0(t_i - \tau_0)]$ and $\varphi_3(t_i) = \sin[\omega_0(t_i - \tau_0)]$ ($i = 1, 2, 3...N$). A statistical weighting method has been used to adjust for the effects of too dense data in the analysis process, the expression of the statistical weighting function is $\omega_i = \exp[-c\omega_0^2(t_i - \tau_0)^2]$. The mother function of WWZ is the Morlet wavelet (Foster 1996a; Xie et al. 2002). The Z variable of WWZ is defined as follows:

$$Z = \frac{(N_{\mathrm{eff}} - 3)V_y}{2(V_x - V_y)}, \quad (3)$$

$$N_{\mathrm{eff}} = \frac{[\sum\exp(-2c\omega_0^2(t_i - \tau_0)^2]^2}{\sum\exp(-2c\omega_0^2(t_i - \tau_0)^2}, \quad (4)$$

is the number of valid data points.

$$V_x = \frac{\sum_i \omega_i x^2(t_i)}{\sum_\lambda \omega_\lambda} - \left[\frac{\sum_i \omega_i x(t_i)}{\sum_\lambda \omega_\lambda}\right]^2,$$
$$V_y = \frac{\sum_i \omega_i y^2(t_i)}{\sum_\lambda \omega_\lambda} - \left[\frac{\sum_i \omega_i y(t_i)}{\sum_\lambda \omega_\lambda}\right]^2, \quad (5)$$

are the simulation functions and weighted variables, respectively (Foster 1996a; VanderPlas 2018).

3. Search for a QPO Signal of Astronomical Data

OVRO observed a 15 GHz radio light curve of FSRQ J0153-1153 from 2009 February to 2018 February, a total of 426 data points, and as shown in Figure 1, we can see that there is a

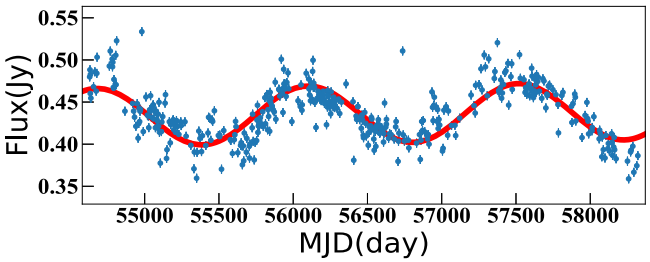

Figure 1. The light curve of FSRQ J0351-1153 is shown from 2009 February to 2018 February. The blue points are the data of the original observations, and the red line are the sine function fits.

periodic signal of this source. In order to quantify the magnitude of light curve variability, we use fractional variability amplitude $F_{\rm var}$ and its error $\sigma_{F_{\rm var}}$, which are calculated as (Edelson et al. 2002; Vaughan et al. 2003; Aleksić et al. 2015):

$$F_{\rm var} = \sqrt{\frac{S^2 - \langle \sigma_{\rm err}^2 \rangle}{\langle f \rangle^2}}, \tag{6}$$

and

$$\sigma_{F_{\rm var}} = \frac{1}{F_{\rm var}} \sqrt{\frac{1}{2N}} \frac{S^2}{\langle f \rangle^2}. \tag{7}$$

Here S^2 is the sample variance, $\langle \sigma_{\rm err}^2 \rangle$ the mean square uncertainty, and $\langle f \rangle$ the average of the fluxes, N indicates the total number of data points (Li et al. 2021). Thus, together with the observed data we obtain $F_{\rm var} = 0.064 \pm 0.031$, which means that the variation of this source is violent during the observation.

3.1. Estimation of Significance Level

Although LSP and WWZ methods are widely used for non-uniformly sampled light curves to search for QPO signals, usually the flux variability of blazars shows frequency-dependent noise behavior, so that the periodograms is likely to cause spurious periods, which can be mistaken for the true periodic component, especially in the lower frequency region (Vaughan et al. 2003; Vaughan 2005; Li et al. 2021). Random fluctuations from stochastic processes are typically modeled by a power spectral density (PSD) of the form $P(f) \propto f^{-\alpha} + C$, in which $P(f)$ denotes PSD, f is in 1/day, α is the slope in PSD, and C denotes positive Poisson noise (Vaughan 2005; Li et al. 2021; Raiteri et al. 2021). The power at time frequency f with a spectral slope of α indicates that the light curves of blazars show a power-law PSD ($\alpha < 0$) with larger oscillations at lower frequencies, resulting in spurious peaks in the periodograms. In particular, the underlying frequency-dependent noise is referred to as red noise ($1 < \alpha < 2$) and flicker noise ($\alpha = 1$), while the flat power spectrum noise ($\alpha = 0$) is referred to as white noise. Therefore, frequency-dependent noise, or colored noise, needs to be carefully considered (Li et al. 2021).

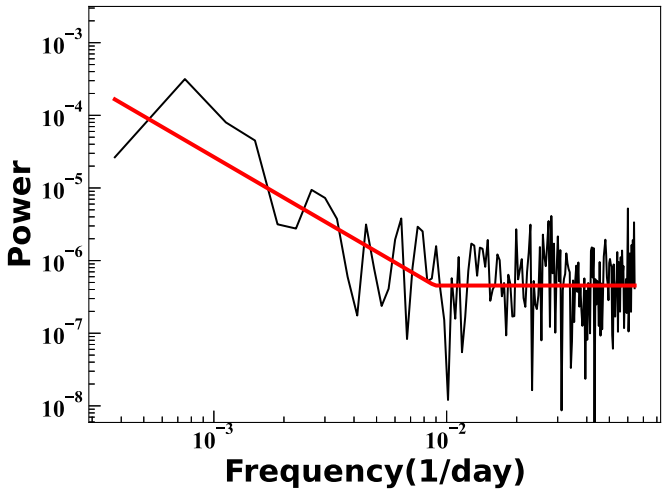

Figure 2. The solid line is the best-fit line, and the slope α of the part of red noise (<0.035 (1/day)) is 1.56 ± 0.26.

Thus, in order to estimate the significance level of the potential QPO signal, we use Timmer & Koenig's method to simulate the light curve (Timmer & Koenig 1995). As shown in Figure 2, the part of the underlying red noise can be modeled a single power law and we estimate the slope α of PSD by fitting a linear function to the log-periodogram using the LSP method following Vaughan's method (Vaughan 2005; Li et al. 2021) and in this case, we take $C = 3$ (the value does not affect the result of the analysis) (Nilsson et al. 2018; Ren et al. 2021a). With $\alpha = 1.56$, we simulate 100,000 light curves with the same variance and the same mean as the original light curve, and the light curves are uniform intervals (Timmer & Koenig 1995). These simulated light curves are analyzed by the LSP method and the WWZ method, respectively (Nilsson et al. 2018; Raiteri et al. 2021). Therefore, we can estimate the significance level of the potential QPO through the PSD of these simulated light curves.

3.2. Analysis Results

In Figure 3, the analysis result of the LSP method is displayed (Zhang et al. 2021). The position indicated by the black arrow is the position where the periodic signal appears, i.e., 7.37×10^{-4} (1/day), and the corresponding periodic signal is 3.72 yr with the significance level of 3.68σ. In Figure 4, the analysis result of the WWZ method is shown. The position indicated by the black arrow is the position where the periodic signal appears, i.e., 7.41×10^{-4} (1/day), and the corresponding periodic signal is 3.69 yr with the significance level of 3.68σ. Here we adopt the average of these two results to be about 3.7 yr and the QPO signal of this source is revealed using these techniques for the first time, and the analysis result of the WWZ also shows that the QPO signal holds steady throughout the observation. Considering

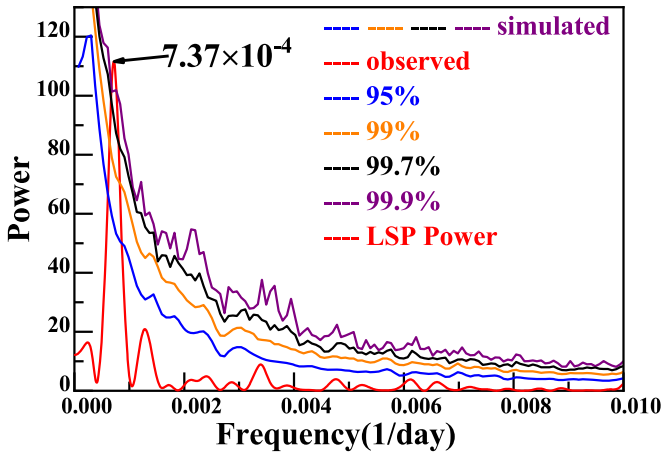

Figure 3. The analysis result of LSP is shown in red line, the purple curve represents the significance level curve in 99.9%, the black curve represents the significance level curve in 99.7%, the orange curve represents the significance level curve in 99%, and the blue curve represents the significance level curve in 95%. The black arrow indicates the position of periodic signals, that is 7.37×10^{-4} (1/day), a counterpart is a 3.72 yr QPO with significance level of 3.68σ.

the analysis result of the LSP, the Gaussian HWHMs at the position of the power peaks provided an uncertainty of 0.5 yr in the measurement observation period, thus the final QPO signal should be 3.7 ± 0.5 yr with a significance level of 3.68σ.

4. Discussion

Based on the above analysis, 3.7 ± 0.5 yr with the significance level of 3.68σ is found in the 15 GHz light curve of FSRQ J0351-1153. This result may reveal some interesting physical phenomena (Timmer & Koenig 1995; Ren et al. 2021a, 2021b). Through the literature previously reported, blazars have a wide range of timescales for QPOs ranging from a few years to a few minutes (Bhatta et al. 2016; Zola et al. 2016; Bhatta 2017). The QPOs include three scales: intra-day variation (IDV) for variations within a day; short-term variation (STV) for variations of several weeks or months; and long-term variation (LTV) for variations of several years (Xiong et al. 2020). The variation on the accretion disk was found to well explain the shorter QPOs in a previous study (Hong et al. 2018; Gupta et al. 2019). For instance, the origin of these orbital motion-related phenomena is explained using hot spots on the accretion disk or non-axisymmetric events around the accretion disk (Hong et al. 2018; Gupta et al. 2019). The long-term QPO is better explained by the jet precession that is caused by the supermassive binary black hole model (Raiteri et al. 2017).

Usually for blazars, the radio radiation generally originates from the synchrotron radiation of relativistic electron in the jet (Chen & Gu 2019). Thus, the physical mechanisms in the jet are first considered when the light curve of radio band is studied. Three possible cases of QPO origin caused by the spiral jet model are discussed in detail by Rieger et al. (Rieger 2004): (1) the orbital-driven spiral motion in a binary black hole leads to an observational QPO larger than 10 d; (2) internal jet rotation leads to observed QPOs less than 10 day; (3) Newtonian-driven jet precession caused by rigid body precessions in the disk may lead to observations of QPOs above 1 yr. According to the above analysis, we have found a 3.7 ± 0.5 yr QPO signal in the 15 GHz radio band for FSRQ J0351-1153. This QPOs timescale is larger than 1 yr; therefore, we consider a Newtonian-driven jet precession to explain this QPO. The Newtonian-drive of the accretion disk has been extensively studied in the literature (Larwood 1998; Kaufman Bernadó et al. 2002). As shown in Figure 5, there is a system of binary black holes orbiting each other, in which we call the primary black hole with accretion disk and relativistic jet, and the relativistic jet is usually perpendicular to the accretion disk and the accretion disk is non-coplanar with the orbiting orbit. A companion black hole exerts a gravitational torque on the accretion disk of the primary black hole, causing the innermost part of the accretion disk to precess periodically; the precession of the accretion disk will be further transmitted to the relativistic jet. Following the diagram below, we discuss in detail the physical origin of this QPO signal.

Romero et al. (2003) have discussed in detail the physical process of QPO signals caused by binary supermassive black holes and have given a relation between the precession period of the jet and the orbital period of the companion star as (Larwood 1998; Romero et al. 2003):

$$\frac{P_{M_2}}{P_{\rm jet}} = \frac{3}{4}\frac{M_2}{M_1}\left(\frac{R_1}{R_2}\right)^{3/2}\left(\frac{M_1}{M_1+M_2}\right)^{1/2}\cos\theta, \quad (8)$$

where P_{M_2} is the orbital period of the companion star and P_{jet} is the precession period of the jet, $\frac{R_1}{R_2} < 1$, thus $\frac{P_{M_2}}{P_{\rm jet}} < 1$. However, considering cosmological expansion and relativistic effects the $P_{\rm obs}$ should be corrected by the following equation (Britzen et al. 2001):

$$P_{\rm jet} = \frac{2\Gamma^2 P_{\rm obs}}{1+z}, \quad (9)$$

In the equation Γ is the Lorentz factor, z is the cosmological redshift, and $P_{\rm obs}$ is the observed QPO signal. Here using the method of Liodakis et al. (2018) Doppler factor δ is equal to 2.52 and the Lorentz factor Γ is equal to 2 for this source. Thus when $\Gamma = 2$ and $P_{\rm obs} = 3.7$ yr we obtain the intrinsic QPO $P_{\rm jet}$ of this source is equal to 11.75 yr. In this system, Romero et al. (2003) studied the system parameters at Doppler factors of 2, 5, and 10, respectively; they found that the mass of the secondary black hole is smaller than that of the primary black hole when the Doppler factor is greater than or equal to 10. Therefore, based on the above analysis, we adopt the average value of the system parameters from Romero et al. (2003) at the Doppler factor equal to 2 as the

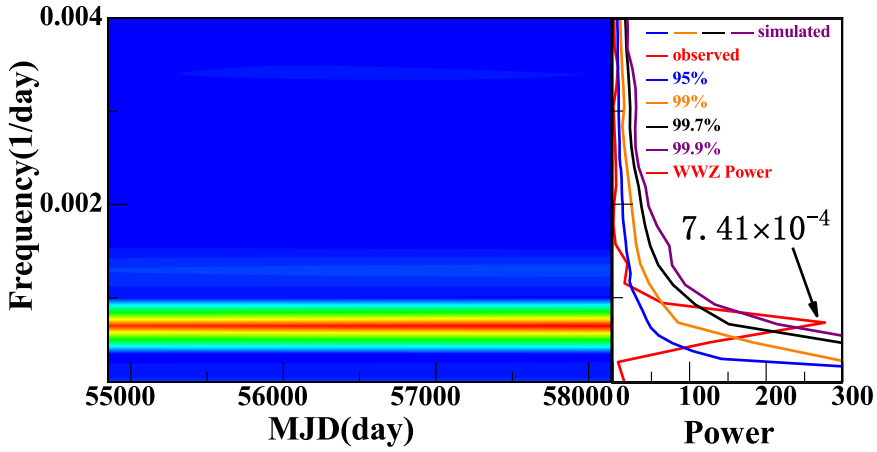

Figure 4. In the left panel, a color plot of WWZ PSD is displayed (red is the strongest, and blue is the weakest). The analysis result of WWZ is shown in the right panel, the purple curve represents the significance level curve in 99.9%, the black curve represents the significance level curve in 99.7%, the orange curve represents the significance level curve in 99%, and the blue curve represents the significance level curve in 95%. In the right panel, the black arrow indicates the position of periodic signals, that is 7.41×10^{-4} (1/day), a counterpart is a 3.69 yr QPO with a significance level of 3.68σ.

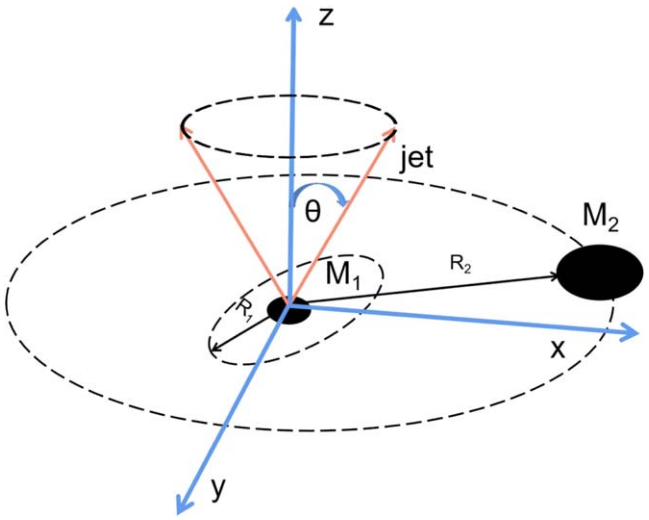

Figure 5. The red arrows represent the relativistic jet carried by the primary black hole, whose direction is usually perpendicular to the accretion disk, and θ is the angular range of the jet oscillation; M_1 is the primary black hole, M_2 is the secondary black hole, R_1 is the radius of the accretion disk precession, and R_2 is the orbital radius of the companion star (Romero et al. 2003).

system parameters of this source. The mass of the primary black hole is $9.2 \times 10^8 M_\odot$, the mass of the secondary black hole is $375.84 \times 10^8 M_\odot$, and $\frac{R_1}{R_2}$ is 0.29, thus P_{M_2} is equal to 8.71 yr. The above analysis shows that periodic flux modulation can be generated when the direction of the jet produces a periodic variation with the direction of the observer's line of sight, therefore we choose an appropriate coordinate system to obtain the following equation (Zhou et al. 2018):

$$\cos(\theta_{\rm obs}) = \sin(\theta)\sin(\phi)\sin(\Omega_{\rm jet} t) + \cos(\theta)\cos(\phi), \quad (10)$$

In which the jet oscillates is in the θ angle range; ϕ is the angle between z-axis and viewer; $\Omega_{\rm jet}$ is the angular velocity of the jet precession ($\Omega_{\rm jet} = \frac{2\pi}{P_{\rm jet}}$) (Sobacchi et al. 2017; Zhou et al. 2018). Of course, we cannot exclude that the QPO signal is caused by other physical mechanisms; for example, in 2019, Zhou et al. found a 34.5 day quasi-periodic signal in the γ-ray of blazars PKS 2247-131, and they found that a helical motion of a blob along the jet is a good explanation to this QPO signal. This geometric motion may also be one of the physical mechanisms that cause this QPO (Zhou et al. 2018). In particular, in 2006 the spin-induced precession of accretion disks gave rise to the precession of jet that caused the periodic signal employed by Reynoso et al. (2006) may be one of the most likely alternative explanations for this QPO signal.

5. Conclusions

In this paper, we study FSRQ J0351-1153 15 GHz band light curve and obtain the following conclusions:

1. For the first time, 3.7 ± 0.5 yr with the significance level of 3.68σ is revealed in FSRQ J0351-1153 utilizing the LSP method, WWZ method and the simulation method for the light curve.
2. By analyzing the Doppler factor of this source it is possible that the mass of the secondary black hole is larger than the mass of the primary black hole, and we also found that the orbital QPO of the secondary black hole is 8.71 yr, while the intrinsic QPO of the precession of the jet is 11.75 yr.
3. Based on the above analysis, we can predict that the next burst in the 15 GHz band should reach its peak brightness in 2024 August.

Acknowledgments

This research has made use of data from the OVRO 40 m monitoring program (Richards, J. L. et al. 2011, ApJS, 194, 29), supported by private funding from the California Institute of Technology and the Max Planck Institute for Radio Astronomy, and by NASA grants NNX08AW31G, NNX11A043G, and NNX14AQ89G and NSF grants AST-0808050 and AST- 1109911. This work is partially supported by the regional first-class discipline of Guizhou province (QJKYF[2018]216), major research projects for innovation groups in Guizhou province (Grant No. KY[2018]028), Electronic Manufacturing Industry-University-Research Base of Ordinary Colleges and Universities in Guizhou Province (Qianjiaohe KY Zi [2014] No. 230-3, Youth Foundation of the Education Department of Guizhou Province (No. KY[2017] 248) and Guizhou Science and Technology Department (QKHJC[2019]1323) and Talent base for R&D of new optoelectronic materials and electronic devices.

References

Abdo, A. A., Ackermann, M., Agudo, I., et al. 2010, ApJ, 716, 30
Ackermann, M., Ajello, M., Albert, A., et al. 2015, ApJL, 813, L41
Aleksić, J., Ansoldi, S., Antonelli, L. A., et al. 2015, A&A, 576, A126
Angel, J. R. P., & Stockman, H. S. 1980, ARA&A, 18, 321
Bhatta, G. 2017, ApJ, 847, 7
Bhatta, G. 2018, Galaxies, 6, 136
Bhatta, G., Zola, S., & Stawarz, Ł. 2016, ApJ, 832, 47
Britzen, S., Roland, J., Laskar, J., et al. 2001, A&A, 374, 784
Chen, Y., & Gu, Q. 2019, Ap&SS, 364, 123
Edelson, R., Turner, T. J., Pounds, K., et al. 2002, ApJ, 568, 610
Esposito, V., Walter, R., Jean, P., et al. 2015, A&A, 576, A122
Foster, G. 1996a, AJ, 111, 541
Foster, G. 1996b, AJ, 112, 1709
Gupta, A. C., Tripathi, A., Wiita, P. J., et al. 2019, MNRAS, 484, 5785
Healey, S. E., Romani, R. W., Taylor, G. B., et al. 2007, ApJS, 171, 61
Hong, S. W., Xiong, D. R., & Bai, J. M. 2017, AJ, 154, 42
Hong, S. W., Xiong, D. R., & Bai, J. M. 2018, AJ, 155, 31
Iyida, E. U., Odo, F. C., Chukwude, A. E., & Ubachukwu, A. A. 2022, NewA, 90, 101666
Kaufman Bernadó, M. M., Romero, G. E., & Mirabel, I. F. 2002, A&A, 385, L10
Larwood, J. 1998, MNRAS, 299, L32
Lee, J. A., Sohn, B. W., Jung, T., Byun, D. -Y., & Lee, J. W. 2017, ApJS, 228, 22
Li, X. -P., Cai, Y., Yang, H.-T., et al. 2021, MNRAS, 506, 1540
Liodakis, I., Hovatta, T., Huppenkothen, D., et al. 2018, ApJ, 866, 137
Lomb, N. R. 1976, Ap&SS, 39, 447
Nilsson, K., Lindfors, E., Takalo, L. O., et al. 2018, A&A, 620, A185
Padovani, P., Resconi, E., Giommi, P., Arsioli, B., & Chang, Y. L. 2016, MNRAS, 457, 3582
Raiteri, C. M., Villata, M., Acosta-Pulido, J. A., et al. 2017, Natur, 552, 374
Raiteri, C. M., Villata, M., Carosati, D., et al. 2021, MNRAS, 501, 1100
Ren, G. W., Ding, N., Zhang, X., et al. 2021a, MNRAS, 506, 3791
Ren, G. W., Zhang, H. J., Zhang, X., et al. 2021b, RAA, 21, 075
Reynoso, M. M., Romero, G. E., & Sampayo, O. A. 2006, A&A, 454, 11
Rieger, F. M. 2004, ApJL, 615, L5
Romero, G. E., Fan, J.-H., & Nuza, S. E. 2003, ChJAA, 3, 513
Scargle, J. D. 1982, ApJ, 263, 835
Sobacchi, E., Sormani, M. C., & Stamerra, A. 2017, MNRAS, 465, 161
Timmer, J., & Koenig, M. 1995, A&A, 300, 707
Tripathi, A., Gupta, A. C., Aller, M. F., et al. 2021, MNRAS, 501, 5997
Urry, C. M., & Padovani, P. 1995, PASP, 107, 803
VanderPlas, J. T. 2018, ApJS, 236, 16
Vaughan, S. 2005, A&A, 431, 391
Vaughan, S., Edelson, R., Warwick, R. S., & Uttley, P. 2003, MNRAS, 345, 1271
Xie, G. Z., Liang, E. W., Zhou, S. B., et al. 2002, MNRAS, 334, 459
Xiong, D. R., Bai, J. M., Fan, J. H., et al. 2020, ApJS, 247, 49
Xiong, D. R., Bai, J. M., Zhang, H. J., et al. 2017, ApJS, 229 21
Zhang, G. Q., Tu, Z. -L., & Wang, F. Y. 2021, ApJ, 909, 83
Zhang, P., & Wang, Z. 2021, ApJ, 914, 1
Zhou, J. N., Wang, Z. X., Chen, L., et al. 2018, NatCo, 9, 4599
Zola, S., Valtonen, M., Bhatta, G., et al. 2016, Galaxies, 4, 41